FRP-confined Concrete Cylinders: Axial Compression Experiments and Strength Model

RIAD BENZAID,[1,2,*] HABIB MESBAH[1] AND NASR EDDINE CHIKH[2]

[1]*Department of Civil Engineering, L.G.C.G.M. Laboratory, INSA de Rennes, 20 Av. des Buttes de Coesmes – 35043 – Rennes cedex, France*

[2]*Department of Civil Engineering, L.M.D.C. Laboratory, Mentouri University – Constantine, Route Ain El Bey Constantine 25000, Algeria*

ABSTRACT: The present article deals with the analysis of experimental results, in terms of load-carrying capacity and strain, obtained from tests on plain- and reinforced-concrete (RC) cylinders strengthened with external carbon-fiber-reinforced polymer (CFRP). The parameters considered are the number of composite layers and the compressive strength of unconfined concrete. The effective circumferential FRP failure strain and the effect of the effective lateral confining pressure were investigated. In total, 30 cylinders were subjected to axial compression, which included control specimens. All the test specimens were loaded to failure in axial compression and the behavior of the specimens in the axial and transverse directions was investigated. Test results showed that the CFRP wrap increases the strength and ductility of plain- and RC cylinders significantly. A simple model is presented to predict the compressive strength and axial strain of FRP-confined columns.

KEY WORDS: concrete column, CFRP, confinement, compressive strength, ultimate strain.

INTRODUCTION

IN RECENT YEARS, the use of externally applied fiber-reinforced polymers (FRP) has gained significant popularity for strengthening and repair of concrete structures. The FRP composites have been used successfully for rehabilitation and upgrading of deficient reinforced-concrete (RC) structures such as buildings, bridges, parking garages, chimneys, etc. One important application of this composite retrofitting technology is the use of FRP jackets to provide external confinement to RC columns when the existing internal transverse reinforcement is inadequate. RC columns need to be laterally confined in order to ensure large deformation under load before failure and to provide an adequate resistance capacity. In the case of a seismic event, energy dissipation allowed by a well-confined concrete core can often save lives. On the contrary, a poorly confined concrete column behaves in a brittle manner leading to sudden and catastrophic failures.

*Author to whom correspondence should be addressed. E-mail: benzaid_riad@yahoo.fr

Figures 3–5 appear in color online: http://jrp.sagepub.com

0731-6844/10/16 2469–20 $10.00/0 DOI: 10.1177/0731684409355199
© The Author(s), 2010. Reprints and permissions:
http://www.sagepub.co.uk/journalsPermissions.nav

The confinement of concrete columns is thus an application where the external wrapping by glass or carbon-fiber-reinforced polymers (CFRP) is particularly effective [1,2]. This innovative technique is already used for reinforcing various types of structures in the civil engineering field. The significance of this subject is confirmed by the numerous experimental researches devoted to the investigation of this mechanism [1–13,17,18,20–26,28,31,36,39,41–44]. Another attractive advantage of FRP over steel straps as external reinforcement is its easy handling, thus minimal time and labor are required to implement them [1].

Focusing the attention on the behavior of compression members, the main parameters investigated in literature [5–13] are the type of FRP material (carbon, aramid, glass, etc.) and its manufacture (unidirectional or bidirectional wraps), the shape of the transverse cross section of the members, the dimensions and shape of the specimens, the strength of concrete, and the types and percentages of steel reinforcements.

Research Significance

The use of externally bonded FRP composite for strengthening and repair can be a cost-effective alternative for restoring or upgrading the performance of existing RC columns. Even though a lot of research has been directed towards circular plain concrete columns, relatively less work has been performed on RC columns to examine the effects of FRP confinement on the structural performance of RC elements. However, all columns in buildings are in reinforced concrete. This article should provide a better understanding of the behavior of RC columns confined with FRP composites. Their strength and rehabilitation need to be given attention to preserve the integrity of building infrastructure. This article is directed towards this endeavor.

Aims and Scope

The main endeavor of this research is to experimentally scrutinize the effects of upgrading the load-carrying capacity of confined circular concrete columns subjected to axial compression by jacketing with CFRP flexible wraps. The objectives of the study are as follows: (1) to evaluate the effectiveness of external CFRP strengthening for circular plain- and RC cylinders; (2) to evaluate the effect of the number of CFRP layers on the ultimate strength and ductility of confined concrete; (3) to evaluate the effect of the original (unconfined) concrete compressive strength on the confinement effectiveness of circular CFRP jackets; and (4) to investigate the effective circumferential FRP failure strain and the effect of the effective lateral confining pressure. A simple confinement model is suggested for FRP-confined columns.

OBSERVED BEHAVIOR OF FRP-CONFINED CYLINDERS

The confinement action exerted by the FRP on the concrete core is of the passive type, that is, it arises as a result of the lateral expansion of concrete under axial load. As the axial stress increases, the corresponding lateral strain increases and the confining device develops a tensile hoop stress balanced by a uniform radial pressure, which reacts against the concrete lateral expansion [14,15]. When an FRP-confined cylinder is subject to axial compression, the concrete expands laterally and this expansion is restrained by the FRP.

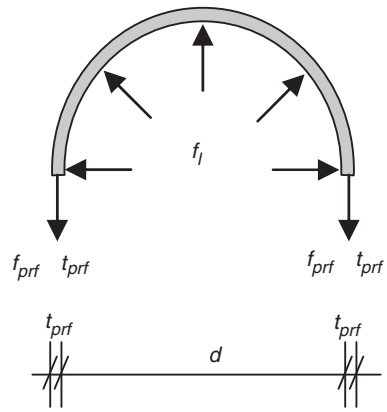

Figure 1. *Confinement action of FRP composite.*

The confining action of the FRP composite for circular concrete columns is shown in Figure 1. For circular columns, the concrete is subject to uniform confinement, and the maximum confining pressure provided by the FRP composite is related to the amount and strength of FRP and the diameter of the confined concrete core. The maximum value of the confinement pressure that the FRP can exert is attained when the circumferential strain in the FRP reaches its ultimate strain and the fibers rupture leading to brittle failure of the cylinder. This confining pressure is given by:

$$f_l = \frac{2\,t_{frp}E_{frp}\varepsilon_{fu}}{d} = \frac{2\,t_{frp}f_{frp}}{d} = \frac{\rho_{frp}f_{frp}}{2}, \tag{1}$$

where f_l is the lateral confining pressure, E_{frp} is the elastic modulus of the FRP composite, ε_{fu} is the ultimate FRP tensile strain, f_{frp} is the ultimate tensile strength of the FRP composite, t_{frp} is the total thickness of the FRP, d is the diameter of the concrete cylinder, and ρ_{frp} is the FRP volumetric ratio. The FRP volumetric ration is given by the following equation for fully wrapped circular cross section:

$$\rho_{frp} = \frac{\pi\,d\,t_{frp}}{\pi\,d^2/4} = \frac{4\,t_{frp}}{d}. \tag{2}$$

DIFFERENT BEHAVIOR BETWEEN STEEL AND FRP COMPOSITES

It is well known that concrete expands laterally before failure. If the lateral expansion is prevented, a substantial concrete strength and deformation enhancements may be gained. Thus, the expected enhancement in the axial load capacity of the columns wrapped with FRP may be due to two factors: first, the confinement effect of the externally bonded transverse fibers; and second, the direct contribution of longitudinally aligned fibers.

Different behavior between steel and FRP composites was observed due to the stress–strain relationship of each material as shown in Figure 2 [16]. FRP is linear elastic up to final brittle rupture when subject to tension while steel has an elastic-plastic region.

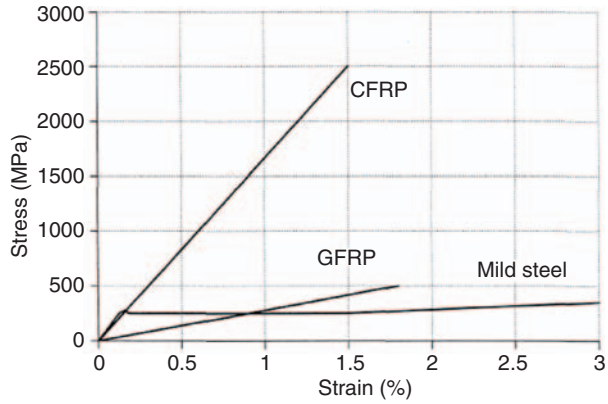

Figure 2. *Typical FRP and mild-steel stress–strain curves [16].*

This is a very important property in terms of structural use of FRP composites. These materials do not possess the ductility that steels have, and their brittleness may limit the ductile behavior of RC members strengthened with FRP composites. Nevertheless, when used to provide confinement for concrete, these materials can greatly enhance the strength and ductility of columns.

EXPERIMENTAL PROGRAM

Material Properties

CONCRETE MIXTURES

Three concrete mixtures were used to achieve the desired range of unconfined concrete strength, as shown in Table 1. Mixtures were prepared in the laboratory using a mechanical mixer.

FRP MATERIAL

The carbon fiber sheets used in this study were the SikaWrap-230C product, a unidirectional wrap. The manufacturer's guaranteed tensile strength for this carbon fiber is 4300 MPa, with a tensile modulus of 238 GPa, ultimate elongation of 18%, and a sheet thickness of 0.13 mm. The resin system that was used to bond the carbon fabrics over the cylinders in this work was the epoxy resin made of two-parts, resin and hardener. The mixing ratio of the two components by weight was 4 : 1. The properties of the resin are given in Table 2 (data are given by the manufacturer). SikaWrap-230C was field laminated using Sikadur-330 epoxy to form a CFRP wrap used to strengthen the concrete specimens.

The mechanical properties, including the modulus and the tensile strength of the CFRP composite jackets, were obtained through tensile testing of flat coupons. The tensile tests were conducted essentially following the NF EN ISO 527-(1, 2, and 5) recommendations [17–19]. The tensile specimen configuration is represented in Figure 3. All of the tests coupons were allowed to cure in the laboratory environment for at least seven days. Prior to the testing, aluminum plates were glued to the ends of the coupons to avoid premature failure of the coupon ends, which were clamped in the jaws of the testing machine.

Table 1. Concrete mixture proportions.

Mixture no.	I	II	III
Compressive cylinder strength, f'_{co} (MPa)	25.93	49.46	61.81
Cement (kg/m^3)	280[a]	400[b]	450[c]
Water (kg/m^3)	180	183.86	170
Crushed gravel (kg/m^3)			
Ø 4/6	122.90	115.70	115.60
Ø 6/12	258.20	243.00	242.80
Ø 12/20	769.50	724.20	723.50
Sand Ø 0/4 (kg/m^3)	729.10	686.30	685.60
Sika Viscocrete-Tempo12(l/m^3),[d]	–	0.85	1.55
Air content (%)	2.30	2.50	2.70
W/C	0.64	0.46	0.37

[a]Portland cement: CPA CEM II R 32.5 MPa.
[b]Portland cement: CPA CEM I R 42.5 MPa.
[c]Portland cement: CPA CEM I R 52.5 MPa.
[d]Sika Viscocrete-Tempo 12: High-range water reducing and super-plasticizing admixture.

Table 2. Properties of the resin Sikadur-330 supplied by manufacturer.

Density about	1.3 at 20°C
Ultimate elongation	0.9% after 7 days at 23°C
Tensile strength	30 MPa after 7 days at 23°C
Tensile modulus	4500 MPa after 7 days at 23°C
Flexural modulus	3800 MPa after 7 days at 23°C
Temperature resistance	exposure continues until 50°C

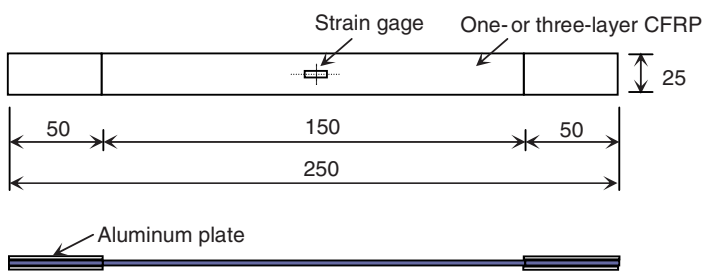

Figure 3. *Flat coupon tensile tests.*

The tests were carried out under displacement control at a rate of 1 mm/min. The longitudinal strains were measured using strain gages at mid-length of the test coupon. The load and strain readings were taken using a data logging system and were stored in a computer. Main mechanical properties obtained from the average values of three tensile coupon tests are summarized as follows:

– Thickness (per ply): 1 mm
– Modulus E_{frp}: 34 GPa
– Tensile strength f_{frp}: 450 MPa
– Ultimate strain ε_{fu}: 14‰

Table 3. Details of test specimens.

Concrete mixture	Specimen code	Description	Unconfined concrete strength (MPa)	No. of specimens
	RCC. 0L	Unconfined		2
	RCC. 1L	One layer		2
I (26 MPa)	RCC. 3L	Three layer	25.93	2
	PCC. 0L	Unconfined		2
	PCC. 1L	One layer		1
	PCC. 3L	Three layer		1
	RCC. 0L	Unconfined		2
	RCC. 1L	One layer		2
II (50 MPa)	RCC. 3L	Three layer	49.46	2
	PCC. 0L	Unconfined		2
	PCC. 1L	One layer		1
	PCC. 3L	Three layer		1
	RCC. 0L	Unconfined		2
	RCC. 1L	One layer		2
III (62 MPa)	RCC. 3L	Three layer	61.81	2
	PCC. 0L	Unconfined		2
	PCC. 1L	One layer		1
	PCC. 3L	Three layer		1

RCC: reinforced concrete cylinder; PCC: plain concrete cylinder; L: layer(s).

Note that the tensile strength was defined based on the cross-sectional area of the coupons, while the elastic modulus was calculated from the stress–strain response.

Specimen Preparation

The experimental program was conducted in the Department of Civil Engineering (I.U.T University of Rennes 1) laboratory. Six series of experiments were performed to investigate the behavior of plain- and RC cylinders confined by CFRP composite. The dimensions of the cylindrical specimens were 160 mm in diameter and 320 mm in height. For all RC specimens the diameter of longitudinal and transverse reinforcing steel bars were respectively 12 and 8 mm. The steel ratio of longitudinal reinforcement was constant for all cylinders and equal to 2.25% (4HA12 mm), with the yield stress being 500 MPa. Transverse ties were spaced every 140 mm (three ties per specimen), with the yield stress being 235 MPa. Series definition and details are given in Table 3.

FRP Wrapping

After 28 days of curing, FRP jackets were applied to the specimens by hand lay-up of CFRP wrap with an epoxy resin. The resin system used in this work was made of two parts, namely, resin and hardener. The components were thoroughly mixed with a mechanical agitator for at least 3 min. The concrete cylinders were cleaned and completely dried before the resin was applied. The mixed Sikadur-330 epoxy resin was directly applied onto the substrate at a rate of 0.7 kg/m^2. The fabric was carefully placed into the resin with gloved hands and any irregularities or air pockets were smoothened out using a plastic

laminating roller. The roller was continuously used until the resin was reflected on the surface of the fabric, an indication of full wetting. After the application of the first wrap of the CFRP, a second layer of resin at a rate of $0.5\,kg/m^2$ was applied on the surface of the first layer to allow the impregnation of the second layer of the CFRP. The third layer was made in the same way. Finally, a layer of resin was applied on the surface of wrapped cylinders. This system is a passive type in that tensile stress in the FRP is gradually developed as concrete expands under the axial load. This expansion is confined by the FRP jacket, which is loaded in tension in the hoop direction. The last CFRP layer was wrapped around the cylinder with an overlap of the 1/4 of perimeter to avoid sliding or debonding of fibers during tests and to ensure the development of full composite strength [20]. The wrapped cylinder specimens were left at room temperature for one week for the epoxy to harden adequately before testing.

Test Setup and Test Procedures

Specimens were loaded under a monotonic uniaxial compression load up to failure. The compressive load was applied at a rate corresponding to 0.24 MPa/s and was recorded with an automatic data acquisition system. Axial and lateral strains were measured using appreciable extensometer. The instrumentation included one radial linear variable differential transducer (LVDT) placed in the form of a hoop at the mid-height of the specimens. Measurement devices also included three vertical LVDTs to measure the average axial strains. Prior to testing, all CFRP-wrapped cylinders as well as the plain concrete cylinders, were capped with sulfur mortar at both ends.

TEST RESULTS AND DISCUSSION

Overall Behavior

The mechanical behavior of the CFRP-wrapped cylinders was very similar in each series in terms of stress–strain curves and failure modes of the specimens. The result (mean-values) listed in Table 4 shows that carbon fiber composite confinement can significantly enhance the ultimate strengths and strains of both plain- and RC cylinders. The ultimate stresses and strains increase with the number of composite layers. For low-strength RC cylinders (26 MPa) confined with CFRP composite, the one-layer specimen exhibited an increase of 69% and 306% in terms of compressive strength and axial strain over the reference specimen, respectively. The three-layer specimen performed better as it recorded an increase in compressive strength and axial strain of 141% and 509%, respectively. However, in high-strength RC cylinders (62 MPa), the gains in strength and strain are much less than those observed in the case of low strength RC cylinders. In this series, the one-layer specimen exhibited an increase of 20% and 39% in terms of compressive strength and axial strain, respectively. The three-layer specimen exhibited an increase in compressive strength and axial strain of 50% and 129%, respectively. The average values of peak strength and corresponding axial and lateral strain are reported in Table 4.

Table 4. Mean-values of experimental results.

Concrete mixture	No. of specimens	Specimen code	f'_{co} (MPa)	f'_{cc} (MPa)	f'_{cc}/f_{co}	ε_{cc} (‰)	$\varepsilon_{cc}/\varepsilon_{co}$	$\varepsilon_{h,rup.}$ (‰)	$\varepsilon_{h,rup.}/\varepsilon_{ho}$
	2	I.RCC.0L		29.51	1	3.77	1	4.95	1
	2	I.RCC.1L	29.51	49.88	1.69	15.34	4.06	13.15	2.65
	2	I.RCC.3L		71.35	2.41	22.98	6.09	13.24	2.67
I (26 MPa)	2	I.PCC.0L		25.93	1	2.73	1	1.77	1
	1	I.PCC.1L	25.93	39.63	1.52	12.78	4.68	13.12	7.41
	1	I.PCC.3L		66.14	2.55	15.16	5.55	13.18	7.44
	2	II.RCC.0L		58.24	1	3.02	1	5.05	1
	2	II.RCC.1L	58.24	77.51	1.33	8.36	2.76	13.16	2.60
II (50 MPa)	2	II.RCC.3L		100.41	1.72	13.58	4.49	13.18	2.61
	2	II.PCC.0L		49.46	1	1.69	1	1.33	1
	1	II.PCC.1L	49.46	52.75	1.06	2.52	1.49	2.90	2.18
	1	II.PCC.3L		82.91	1.67	7.27	4.30	13.15	9.88
	2	III.RCC.0L		63.01	1	2.69	1	4.90	1
	2	III.RCC.1L	63.01	76.21	1.20	3.75	1.39	5.20	1.06
III (62 MPa)	2	III.RCC.3L		94.81	1.50	6.18	2.29	5.62	1.14
	2	III.PCC.0L		61.81	1	2.84	1	2.40	1
	1	III.PCC.1L	61.81	62.68	1.01	3.27	1.15	2.46	1.02
	1	III.PCC.3L		93.19	1.50	10.54	3.71	12.89	5.37

Stress–Strain Response

The measured stress–strain curves for the CFRP-wrapped cylinders are shown in Figure 4. The figures give the axial stress vs. the axial and lateral strains for plain- and RC specimens with zero, one, and three layers of CFRP wrap. For low-strength reinforced-concrete (26 MPa) confined with CFRP composite the stress–strain curves showed a typical bilinear trend with strain hardening similar to that of the CFRP-confined plain concrete cylinders (Figure 4(a) and (b)). Typically, three zones can be observed for the stress–strain curves of the CFRP-confined cylinders. The first zone is essentially a linear response governed by the stiffness of the unconfined concrete, which indicates that no confinement is activated in the CFRP wraps since the lateral strains in the concrete are very small. In the second zone, a non-linear transition occurs as the concrete expands, thus producing larger lateral strains. The CFRP wrap reacts accordingly and a confining action is created on the concrete core. During this stage, a loss of stiffness occurs due to the rapidly growing network of cracks in the concrete. Finally, in the third zone, the concrete is fully cracked and the CFRP confinement is activated to provide additional load-carrying capacity by keeping the concrete core intact. The stress–strain curve here increases linearly up to failure. The stiffness of the specimen in this zone depends on the modulus of elasticity of the CFRP material and on the level of confinement. As already mentioned, FRP stress–strain behavior is essentially linear elastic up to failure, which explains the linearity of the third zone. With this type (the increasing type) of stress–strain curves, both the compressive strength and the ultimate strain are reached at the same point and are significantly enhanced.

However, in higher strength concrete (50 and 62 MPa) as the unconfined concrete strength increases, the second part of the bilinear curve shifts from strain hardening to a flat plateau, and eventually to a sudden strain softening with drastically reduced ductility (Figure 4(c)–(f)). As the stress–strain curve terminates at a concrete stress f'_{cu} (stress in concrete at the ultimate strain) above the compressive strength of unconfined concrete f'_{co}

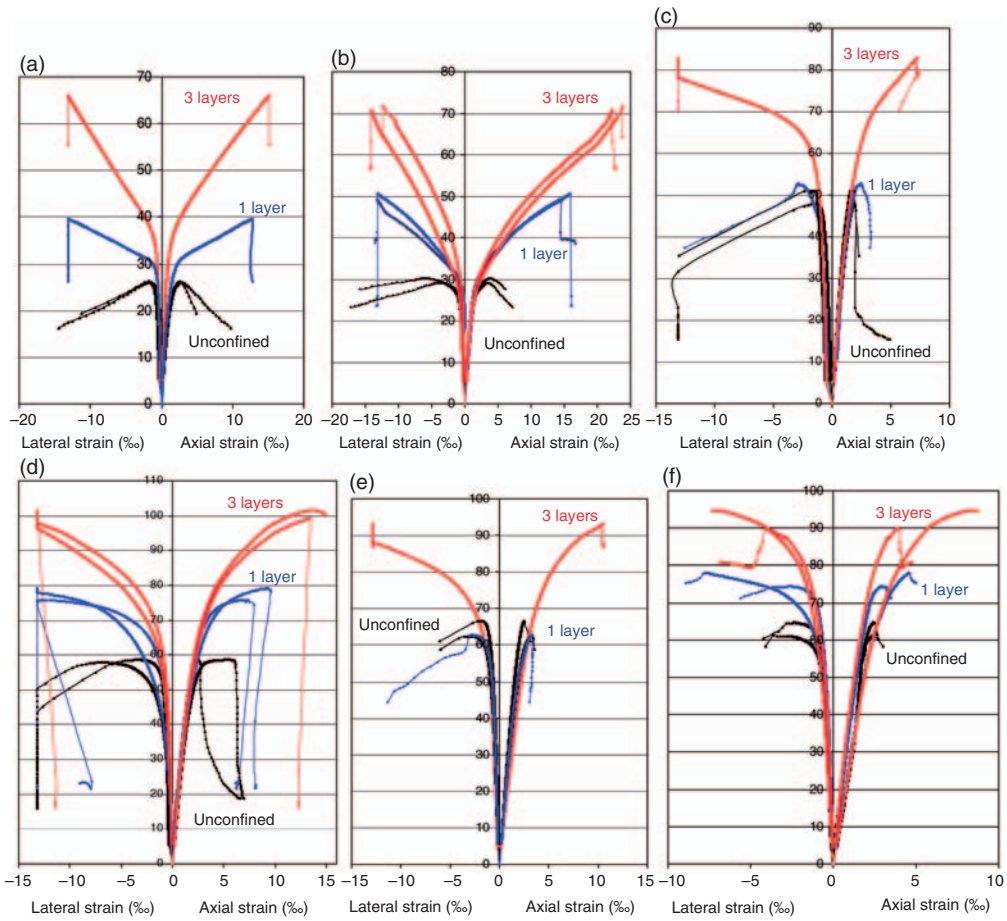

Figure 4. *Experimental stress–strain curves of fiber-reinforced polymer-wrapped concrete cylinders: (a) plain concrete (f'_{co} = 26 MPa); (b) reinforced concrete (f'_{co} = 26 MPa); (c) plain concrete (f'_{co} = 50 MPa); (d) reinforced concrete (f'_{co} = 50 MPa); (e) plain concrete (f'_{co} = 62 MPa); and (f) reinforced concrete (f'_{co} = 62 MPa).*

as illustrated in Figure 4(e) (one-layer confined specimens), the FRP confinement is still sufficient to lead to strength enhancement.

From the trends shown in Figure 4(e) (62 MPa), it is clear that, unlike low-strength concrete, in higher strength concrete confining the cylinders with one layer of CFRP wrap does not significantly change the stress–strain behavior of confined concrete from that of unconfined concrete except for a very limited increase in compressive strength (e.g., 1% for III.PCC.1L specimen), see Table 4. In that case the stress–strain curve terminates at a stress $f'_{cu} < f'_{co}$, the specimen is said to be insufficiently confined, where little strength enhancement can be expected. Whereas, for a high level of confinement, cylinder confined with three CFRP layers, both the compressive strength and the ultimate strain are significantly enhanced.

On the light of the results indicated in Table 4, it can be concluded that: the CFRP confinement on low-strength concrete specimens produced higher results in terms of strength and strains than for high-strength concrete similar specimens.

Figure 5. *Typical failure modes of CFRP-confined concrete cylinders: (a) f'_{co} = 26 MPa; (b) f'_{co} = 50 MPa; and (c) f'_{co} = 62 MPa.*

Failure Mode

All the CFRP-wrapped cylinders failed by the rupture of the FRP jacket due to hoop tension. The CFRP-confined specimens failed in a sudden and explosive manner and were only preceded by some snapping sounds. Many hoop sections formed as the CFRP ruptured. These hoops were either concentrated in the central zone of the specimen or distributed over the entire height, as can be seen in Figure 5. The wider the hoop, the greater the section of concrete that remained attached to the inside face of the delaminated CFRP. None of the specimens failed at the overlap location of the jacket, which confirmed the adequate stress transfer over the splice.

PROPOSED MODEL

Ultimate Strength of FRP-confined Concrete Cylinders

EXISTING MODELS

Various models for confinement of concrete with FRP have been developed. The majority of these models were performed on plain concrete specimens' tests. A limited number of tests have been reported in the literature on the axial compressive strength and strain of RC specimens confined with FRP. Most of the existing strength models for FRP-confined concrete adopted the concept of Richart et al. [21], in which the strength at failure for concrete confined by hydrostatic fluid pressure takes the following form:

$$f'_{cc} = f'_{co} + k_1 \cdot f_l, \tag{3}$$

where f'_{cc} and f'_{co} are the compressive strength of confined and the unconfined concrete respectively, f_l is the lateral confining pressure and k_1 is the confinement effectiveness coefficient. In applying their model to steel-confined concrete, Richart et al. [21] assumed that k_1 is a constant equal to 4.1. However, several studies revealed that existing models for the axial compressive strength of steel-confined concrete are un-conservative and cannot be used for FRP-confined concrete (see [6,16,22–26], among others). Many authors have raised towards the steel-based confinement models the objection that they do not account for the profound difference in uniaxial tensile stress–strain behavior between steel and FRP. According to these authors, while the assumption of constant confining pressure is still realistic in the case of steel confinement in the

Table 5. Average hoop rupture strain ratios.

Concrete mixture	Specimen code	ε_{fu} (‰)	$\varepsilon_{h.rup.}$ (‰)	$\varepsilon_{h.rup.}/\varepsilon_{fu}$
I (26 MPa)	I.RCC.1.1L	14	13.15	0.939
	I.RCC.2.1L	14	13.16	0.940
	I.RCC.1.3L	14	14.06	1.004
	I.RCC.2.3L	14	12.42	0.887
	I.PCC.1.1L	14	13.12	0.937
	I.PCC.1.3L	14	13.18	0.941
II (50 MPa)	II.RCC.1.1L	14	13.17	0.940
	II.RCC.2.1L	14	13.16	0.940
	II.RCC.1.3L	14	13.20	0.942
	II.RCC.2.3L	14	13.17	0.940
	II.PCC.1.1L	14	2.90	0.207
	II.PCC.1.3L	14	13.15	0.939
III (62 MPa)	III.RCC.1.1L	14	7.79	0.556
	III.RCC.2.1L	14	2.61	0.186
	III.RCC.1.3L	14	4.10	0.292
	III.RCC.2.3L	14	7.15	0.510
	III.PCC.1.1L	14	2.46	0.175
	III.PCC.1.3L	14	12.89	0.920

yield phase, it cannot be extended to FRP materials, which do not exhibit any yielding and therefore apply on the concrete core a continuously increasing inward pressure. However, a number of strength models have been proposed specifically for FRP-confined concrete that employ Equation (3) with modified expressions for k_1, (e.g., [6,22,23,25–37]). Most of these models used a constant value for k_1 (between 2 and 3.5) indicating that the experimental data available in the literature show a linear relationship between the strength of confined concrete f'_{cc} and the lateral confining pressure f_l [29–37]. Other researchers expressed k_1 in non-linear form in terms of f_l/f'_{co} or f_l [6,22,23,25–28].

FRP CIRCUMFERENTIAL FAILURE STRAIN

According to the obtained test results, cylinder failure occurs before the FRP reached their ultimate strain capacities ε_{fu}. So the failure occurs prematurely and the circumferential failure strain was lower than the ultimate strain obtained from standard tensile testing of the FRP composite. This phenomenon considerably affects the accuracy of the existing models for FRP-confined concrete. Referring to Table 5, for example, the rupture of the low-strength cylinder IRCC.2.3L corresponded to a maximum composite extension (circumferential failure strain) $\varepsilon_{h,rup}$ of 12.42‰ which is lower than the ultimate composite strain ε_{fu} (14‰) as it represents about 88% of it. This reduction in the strain of the FRP composites can be attributed to several causes as reported in related literature [25,32,38]:

–The curved shape of the composite wrap or misalignment of fibers may reduce the FRP axial strength;
–Near failure the concrete is internally cracked resulting in non-homogeneous deformations. Due to this non-homogeneous deformations and high loads applied on the cracked concrete, local stress concentrations may occur in the FRP reinforcement.

EFFECTIVE FRP STRAIN COEFFICIENT

In existing models for FRP-confined concrete, it is commonly assumed that the FRP ruptures when the hoop stress in the FRP jacket reaches its tensile strength from either flat coupon tests which is herein referred to as the FRP material tensile strength. This assumption is the basis for calculating the maximum confining pressure f_l (the confining pressure reached when the FRP ruptures) given by Equation (1). The confinement ratio of an FRP-confined specimen is defined as the ratio of the maximum confining pressure to the unconfined concrete strength (f_l/f'_{co}).

However, experimental results show that the FRP material tensile strength was not reached at the rupture of FRP in FRP-confined concrete. Table 5 provides the average ratios between the measured circumferential strain at FRP rupture ($\varepsilon_{h,rup}$) and the ultimate tensile strain of the FRP material (ε_{fu}). It is seen that, when all specimens of the present study are considered together, the average ratio ($\varepsilon_{h,rup}/\varepsilon_{fu}$) has a value closer to 0.73 and is referred to, in this article, as the effective FRP strain coefficient η. Thus, the maximum confining pressure given by Equation (1) can be considered as a nominal value. The effective maximum lateral confining pressure is given by:

$$f_{l\text{eff}} = \frac{2\,t_{frp}E_{frp}\varepsilon_{h,rup}}{d} = \frac{2\,t_{frp}E_{frp}\eta\varepsilon_{fu}}{d} = \eta f_l. \tag{4}$$

Table 5 indicates that the assumption that the FRP ruptures when the stress in the jacket reaches the FRP material tensile strength is invalid for concrete confined by FRP wraps.

PARAMETERS FOR CONFINEMENT EFFECT

The actual confinement ratio ($f_{l,eff}/f'_{co}$) of FRP confined concrete is defined as a ratio of the effective lateral confining pressure to the unconfined concrete strength. Strengthening ratio or confinement effectiveness (f'_{cc}/f'_{co}) is defined as the ratio between the strength of confined concrete to that of unconfined concrete, that measures how effectively the concrete is confined in a given cross section. The main parameters that are likely to influence the confinement effect are the volumetric ratio of FRP, tensile strength of FRP in hoop direction, and the strength of unconfined concrete. The effect of confinement on these parameters was determined based on the test results. The peak strength f'_{cc} of the confined concrete depends on the value of the effective lateral confinement pressure $f_{l,eff}$.

PROPOSED EQUATION

A simple equation is proposed to predict the peak strength of FRP-confined concrete of different unconfined strengths based on regression of test data reported in Table 6. Figure 6 shows the relation between actual confinement ratio $f_{l,eff}/f'_{co}$ and the strengthening ratio f'_{cc}/f'_{co} for the cylinders of the test series. It can be seen that, strengthening ratio is proportional to the volumetric ratio and the strength of FRP (in terms of effective lateral confining pressure $f_{l,eff}$) and is inversely proportional to unconfined concrete strength. Therefore the relationship may be approximated by a linear function. The trend line of these test data can be closely approximated using the following equation:

$$\frac{f'_{cc}}{f'_{co}} = 1 + 2.20\frac{f_{l\text{eff}}}{f'_{co}}. \tag{5}$$

Table 6. Data and results of CFRP wrapped cylinders.

Concrete mixture	Specimen code	f'_{co} (MPa)	t (mm)	E (GPa)	ε_{fu} (‰)	$\varepsilon_{h.rup.}$ (‰)	d (mm)	$f_{l.eff}$ (MPa)	f_l (MPa)	f_l/f'_{co}	$f_{l.eff}/f'_{co}$	f'_{cc} (MPa)	f'_{cc}/f'_{co}	ε_{co} (‰)	ε_{cc} (‰)	$\varepsilon_{cc}/\varepsilon_{co}$
	I.RCC.1.1L	29.51	1	34	14	13.15	160	5.588	5.95	0.201	0.189	50.59	1.714	3.77	15.93	4.225
	I.RCC.2.1L	29.51	1	34	14	13.16	160	5.593	5.95	0.201	0.189	49.17	1.666	3.77	14.75	3.912
I (26 Mpa)	I.RCC.1.3L	29.51	3	34	14	14.06	160	17.926	17.85	0.604	0.607	70.83	2.400	3.77	22.22	5.893
	I.RCC.2.3L	29.51	3	34	14	12.42	160	15.835	17.85	0.604	0.536	71.88	2.435	3.77	23.74	6.297
	I.PCC.1.1L	25.93	1	34	14	13.12	160	5.576	5.95	0.229	0.215	39.63	1.528	2.73	12.78	4.681
	I.PCC.1.3L	25.93	3	34	14	13.18	160	16.804	17.85	0.688	0.648	66.14	2.550	2.73	15.16	5.553
	II.RCC.1.1L	58.24	1	34	14	13.17	160	5.597	5.95	0.102	0.096	75.84	1.302	3.02	7.37	2.440
	II.RCC.2.1L	58.24	1	34	14	13.16	160	5.593	5.95	0.102	0.096	79.18	1.359	3.02	9.35	3.096
II (50 Mpa)	II.RCC.1.3L	58.24	3	34	14	13.20	160	16.83	17.85	0.306	0.288	101.48	1.742	3.02	13.72	4.543
	II.RCC.2.3L	58.24	3	34	14	13.17	160	16.791	17.85	0.306	0.288	99.35	1.705	3.02	13.44	4.450
	II.PCC.1.1L	49.46	1	34	14	2.90	160	1.232	5.95	0.120	0.024	52.75	1.066	1.69	2.52	1.491
	II.PCC.1.3L	49.46	3	34	14	13.15	160	16.766	17.85	0.360	0.338	82.91	1.676	1.69	7.27	4.301
	III.RCC.1.1L	63.01	1	34	14	7.79	160	3.310	5.95	0.094	0.052	77.99	1.237	2.69	4.59	1.706
	III.RCC.2.1L	63.01	1	34	14	2.61	160	1.109	5.95	0.094	0.017	74.43	1.181	2.69	2.91	1.081
III (62 Mpa)	III.RCC.1.3L	63.01	3	34	14	4.10	160	5.227	17.85	0.283	0.082	94.92	1.506	2.69	3.87	1.438
	III.RCC.2.3L	63.01	3	34	14	7.15	160	9.116	17.85	0.283	0.144	94.71	1.503	2.69	8.49	3.156
	III.PCC.1.1L	61.81	1	34	14	2.46	160	1.045	5.95	0.096	0.016	62.68	1.014	2.84	3.27	1.151
	III.PCC.1.3L	61.81	3	34	14	12.89	160	16.434	17.85	0.288	0.265	93.19	1.507	2.84	10.54	3.711

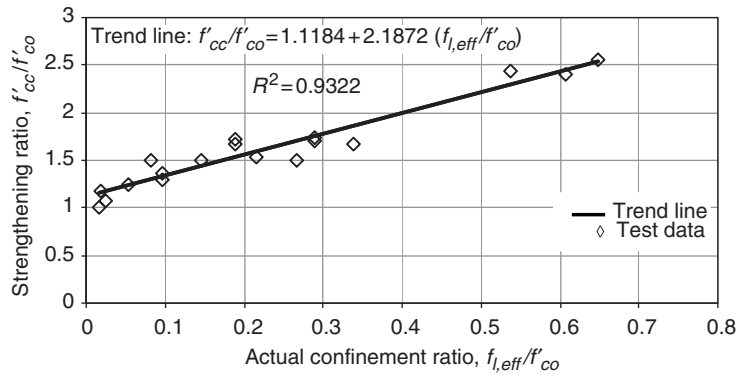

Figure 6. *Strengthening ratio vs. actual confinement ratio.*

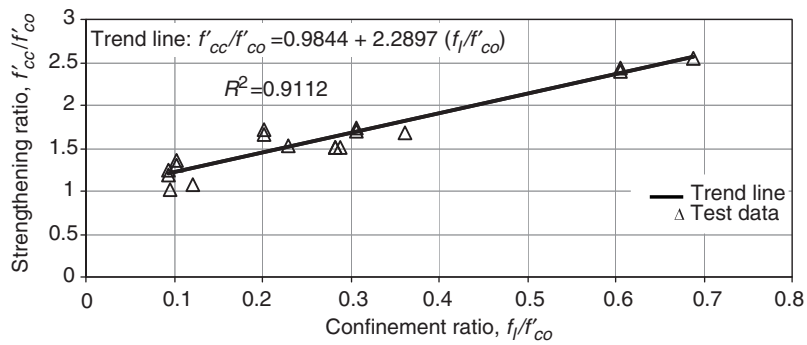

Figure 7. *Strengthening ratio vs. confinement ratio.*

Using a reduction factor η of 0.73 with the replacement of $f_{l,eff}$ by f_l into Equation (5) the ultimate axial compressive strength of FRP-confined concrete takes the form:

$$\frac{f'_{cc}}{f'_{co}} = 1 + 1.60\frac{f_{l,}}{f'_{co}}. \tag{6}$$

Figure 7 is a plot of the strengthening ratio f'_{cc}/f'_{co} against the confinement ratio f_l/f'_{co}. The trend line of this figure shows a much greater average confinement effectiveness coefficient k_1. This can be attributed to the effect of the effective lateral confining pressure.

Ultimate Axial Strain of FRP-confined Concrete Cylinders

EXISTING MODELS

Early investigation showed that for steel confined concrete, the axial compressive strain ε_{cc} at the peak axial stress can be related to the lateral confining pressure [21] by:

$$\varepsilon_{cc} = \varepsilon_{co}\left(1 + k_2\frac{f_l}{f'_{co}}\right), \tag{7}$$

where ε_{co} is the axial strain of the unconfined concrete at its peak stress and k_2 is the strain enhancement coefficient. Richart et al. [21] suggested $k_2 = 5\,k_1$ for steel-confined concrete. For FRP-confined concrete, many studies suggested that ultimate axial strain can also be related to the lateral confining pressure (e.g., [15,25,27,29,32,34,39,40]).

In literature, some methods for predicting the ultimate strain of FRP-confined concrete cylinders have been proposed. Existing models can be classified into three categories as follows:

(a) Steel-based confined models (e.g., [5,41])

From Saadatmanesh et al. [5]:

$$\frac{\varepsilon_{cc}}{\varepsilon_{co}} = 1 + 5\left(\frac{f'_{cc}}{f'_{co}} - 1\right), \tag{8}$$

where ε_{co} is the strain in peak stress of unconfined concrete and ε_{cc} is ultimate strain of FRP-confined concrete.

(b) Empirical or analytical models (e.g., [16,22–24,26,28–30,40,42,43])

From Teng et al. [16]:

–For CFRP wrapped concrete:

$$\frac{\varepsilon_{cc}}{\varepsilon_{co}} = 2 + 15\left(\frac{f_l}{f'_{co}}\right). \tag{9}$$

–For design use:

$$\frac{\varepsilon_{cc}}{\varepsilon_{co}} = 1.75 + 10\left(\frac{f_l}{f'_{co}}\right). \tag{10}$$

(c) Recently, some models for predicting the axial stress and strain of FRP-confined concrete were suggested based on numerical method or plasticity analysis (e.g. [20,44–47]), whereas these models are often not suitable for direct use in design.

PROPOSED EQUATION

Figure 8 shows the relation between the strain enhancement ratio and the actual confinement ratio of the present test data. A linear relationship clearly exists. This diagram indicates that the ultimate strain of FRP-confined concrete can be related linearly to the actual confinement ratio. Based on regression of test data reported in Table 6, the ultimate axial strain of CFRP-wrapped concrete can be approximated by the following expression:

$$\frac{\varepsilon_{cc}}{\varepsilon_{co}} = 2 + 7.6\left(\frac{f_{leff}}{f'_{co}}\right). \tag{11}$$

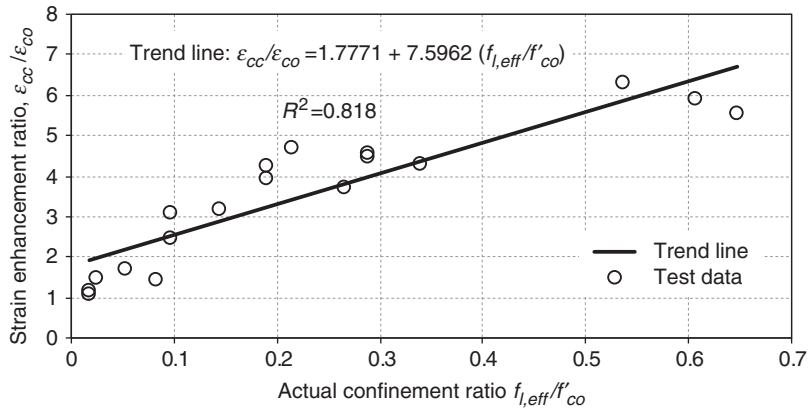

Figure 8. *Strain enhancement ratio vs. actual confinement ratio.*

Table 7. Comparison of experimental and predicted results: compressive strength.

Source	Specimen code	FRP type	f'_{co} (MPa)	E_{frp} (GPa)	ε_{fu} (‰)	t (mm)	d (mm)	f_l (MPa)	k_1	$f'_{cc.theo}$ (MPa)	$f'_{cc,\exp}$ (MPa)	$f'_{cc.theo}/f'_{cc.\exp}$
Matthys et al. [25]	k2	CFRP	32	198	11.9	0.585	400	6.891	1.6	43.027	54.30	0.792
	k8	HFRP	32	120	9.6	0.492	400	2.833	1.6	36.534	44.40	0.822
Ilki et al. [49]	CYL-3-1	CFRP	6.2	230	15	0.495	150	22.770	1.6	42.632	52.20	0.816
	CYL-5-1	CFRP	6.2	230	15	0.825	150	37.950	1.6	66.920	87.70	0.763
	CYL-5-2	CFRP	6.2	230	15	0.825	150	37.950	1.6	66.920	82.70	0.809
Lam and Teng [48]	CI-M1	CFRP	41.1	250	15.2	0.165	152	8.250	1.6	54.300	52.60	1.032
	CI-M2	CFRP	41.1	250	15.2	0.165	152	8.250	1.6	54.300	57.00	0.952
	CI-M3	CFRP	41.1	250	15.2	0.165	152	8.250	1.6	54.300	55.40	0.980
	CII-M3	CFRP	38.9	247	15.2	0.33	152	16.302	1.6	64.983	65.80	0.987
Jiang and Teng [29]	36	CFRP	38	240.7	15	1.02	152	48.456	1.6	115.530	129	0.895
	37	CFRP	38	240.7	15	1.02	152	48.456	1.6	115.530	135.7	0.851
	38	CFRP	38	240.7	15	1.36	152	64.608	1.6	141.374	161.3	0.876
	39	CFRP	38	240.7	15	1.36	152	64.608	1.6	141.374	158.5	0.891
	40	CFRP	37.7	260	15	0.11	152	5.644	1.6	46.731	48.50	0.963
	41	CFRP	37.7	260	15	0.11	152	5.644	1.6	46.731	50.30	0.929
	42	CFRP	44.2	260	15	0.11	152	5.644	1.6	53.231	48.10	1.106
	43	CFRP	44.2	260	15	0.11	152	5.644	1.6	53.231	51.10	1.041
	44	CFRP	44.2	260	15	0.22	152	11.289	1.6	62.263	65.70	0.947
	45	CFRP	44.2	260	15	0.22	152	11.289	1.6	62.263	62.90	0.989
	46	CFRP	47.6	250.5	15	0.33	152	16.315	1.6	73.704	82.70	0.891
										Average		0.917
										Standard deviation		0.092
										Coefficient of variation (%)		10

Table 8. Comparison of experimental and predicted results: ultimate axial strain.

Source	Specimen code	Experimental results		Theoretical results		
		ε_{co}	$\varepsilon_{cc.exp}$	k_2	$\varepsilon_{cc,theo}$	$\varepsilon_{cc.theo}/\varepsilon_{cc.exp}$
Matthys et al. [25]	k2	0.00280	0.0111	5.55	0.0089	0.806
	k8	0.00280	0.0059	5.55	0.0069	1.182
Ilki et al. [49]	CYL-3-1	0.00191	0.0690	5.55	0.0428	0.621
	CYL-5-1	0.00196	0.0910	5.55	0.0707	0.777
	CYL-5-2	0.00203	0.0940	5.55	0.0730	0.777
Lam and Teng [48]	CI-M1	0.00256	0.0090	5.55	0.0079	0.885
	CI-M2	0.00256	0.0121	5.55	0.0079	0.658
	CI-M3	0.00256	0.0111	5.55	0.0079	0.718
	CII-M3	0.00256	0.0125	5.55	0.0110	0.885
Jiang and Teng [29]	36	0.00217	0.0279	5.55	0.0196	0.704
	37	0.00217	0.0308	5.55	0.0196	0.639
	38	0.00217	0.0370	5.55	0.0248	0.670
	39	0.00217	0.0354	5.55	0.0248	0.700
	40	0.00275	0.0089	5.55	0.0077	0.869
	41	0.00275	0.0091	5.55	0.0077	0.851
	42	0.00260	0.0069	5.55	0.0070	1.019
	43	0.00260	0.0088	5.55	0.0070	0.793
	44	0.00260	0.0130	5.55	0.0088	0.681
	45	0.00260	0.0102	5.55	0.0088	0.866
	46	0.00279	0.0130	5.55	0.0108	0.834
				Average		0.797
				Standard deviation		0.134
				Coefficient of variation (%)		17.2

Replacing $f_{l,eff}$ by f_l into Equation (11) the ultimate axial strain of FRP-confined concrete takes the form:

$$\frac{\varepsilon_{cc}}{\varepsilon_{co}} = 2 + 5.55\left(\frac{f_l}{f'_{co}}\right). \tag{12}$$

Validation of the Proposed Model

Using the above model, the compressive strength and axial strain of FRP-confined specimens collected from other studies [25,29,48,49] were predicted, as shown in Tables 7 and 8, which clearly exhibits excellent agreement between the experimental and predicted results.

It should be reminded that, for high-strength concrete ($f'_{co} \geq 50$ MPa) confined by FRP composite with $f_l/f'_{co} \leq 0.095$ the specimen is said to be insufficiently confined. Such concrete is not expected to possess a compressive strength significantly above that of unconfined concrete and the FRP may rupture at a low hoop strain. Such insufficiently confined concrete should not be allowed in design.

CONCLUSIONS

The purpose of the experimental work involved in this study was mainly to evaluate the effectiveness of strengthening plain- and RC cylinders with CFRP composite. Based on the analysis of experimental results, the following conclusions are made:

(1) The experimental results clearly demonstrate that composite wrapping can enhance the structural performance of RC columns under axial loading, in terms of both maximum strength and strain. In general, the confinement effectiveness reduces with an increase in the unconfined concrete strength.
(2) The average hoop strain in FRP at rupture in FRP-wrapped concrete can be much lower than the FRP material ultimate tensile strain supplied by manufacturers, indicating the assumption that FRP ruptures when the FRP material tensile strength reached is not valid in the case of concrete confined by FRP wraps. Based on this observation, an effective peak stress and corresponding strain formula for concrete confined by FRP must be based on the actual hoop rupture strain of FRP rather than the ultimate material tensile strain.
(3) In vast majority of cases, the stress–strain curve of FRP-confined concrete is or can be approximated as a monotonically ascending bilinear curve with a transition zone. The elastic slope is not substantially altered with confinement whereas the plastic rigidity is function of the confinement level. Such FRP-confined concrete is said to be sufficiently confined.
(4) For both plain- and reinforced-concrete confined with FRP composite, the ultimate strengths and strains increase significantly with the number of composites layers.
(5) The thickness and tensile strength of the FRP jacket in the hoop direction significantly influence the confinement effectiveness for low- and high-strength concrete.
(6) Failure of all confined cylinders is marked by the rupture of carbon fibers. It occurs prematurely, for stress level appreciably lower than the ultimate strength of the FRP composite.
(7) Based on the analysis of the experimental results, a simple model has been proposed for the prediction of the ultimate strength and strain of FRP- confined concrete, and a good correlation was obtained between experimental and analytical results.

ACKNOWLEDGMENT

Authors thankfully acknowledge the support of Sika-France S.A (Saint-Gregoire, Rennes) for providing the FRP materials.

REFERENCES

1. Demer, M. and Neale, K. W. (1999). Confinement of Reinforced Concrete Columns with Fibre-reinforced Composite Sheets - An Experimental Study, *Can. J. Civil. Eng.*, **26**(2): 226–241.
2. Rochette, P. and Labossiere, P. (2000). Axial Testing of Rectangular Column Models Confined with Composites, *ASCE J. Compos. Constr.*, **4**(3): 129–136.
3. Berthet, J., Ferrier, E. and Hamelin, P. (2005). Compressive Behavior of Concrete Externally Confined by Composite Jackets. Part A: Experimental Study, *Constr. Build. Mater.*, **19**(3): 223–232.
4. Binici, B. and Mosalam, K. M. (2007). Analysis of Reinforced Concrete Columns Retrofitted with Fiber Reinforced Polymer Lamina, *Compsites Part B*, **38**: 265–276.
5. Saadatmanesh, H., Ehsani, M. R. and Li, M. W. (1994). Strength and Ductility of Concrete Columns Externally Reinforced with Composites Straps, *ACI Struct. J.*, **91**(4): 434–447.
6. Mirmiran, A. and Shahawy, M. (1997). Behavior of Concrete Columns Confined by Fiber Composites, *ASCE J. Struct. Eng.*, **123**(5): 583–590.
7. Theriault, M., Neale, K. W. and Claude, S. (2004). Fiber-reinforced Polymer-Confined Circular Concrete Columns: Investigation of Size and Slenderness Effects, *ASCE J. Compos. Constr.*, **8**(4): 323–331.
8. Kumutha, R., Vaidyanathan, R. and Palanichamy, M. S. (2007). Behaviour of Reinforced Concrete Rectangular Columns Strengthened Using GFRP, *Cem. Concr. Compos.*, **29**: 609–615.

9. Chaallal, O., Hassan, M. and LeBlanc, M. (2006). Circular Columns Confined With FRP: Experimental Versus Predictions of Models and Guidelines, *ASCE J. Compos. Constr.*, **10**(1): 4–12.
10. Almusallam, T. H. (2007). Behavior of Normal and High-strength Concrete Cylinders Confined with E-Glass/Epoxy Composite Laminates, *Composites Part B*, **38**: 629–639.
11. Wang, Y.-C. and Hsu, K. (2008). Design of FRP-wrapped Reinforced Concrete Columns for Enhancing Axial Load Carrying Capacity, *Compos. Struct.*, **82**: 132–139.
12. Wang, L.-M. and Wu, Y.-F. (2008). Effect of Corner Radius on the Performance of CFRP-Confined Square Concrete Columns: Test, *Eng. Struct.*, **30**: 493–505.
13. Benzaid, R., Chikh, N.-E. and Mesbah, H. (2009). Study of the Compressive Behavior of Short Concrete Columns Confined by Fiber Reinforced Composite, *Arab. J. Sci. Eng.*, **34**(1B): 15–26.
14. De Lorenzis, L. and Tepfers, R. (2001). *A Comparative Study of Models on Confinement of Concrete Cylinders with FRP Composites*, Division of Building Technology, Work No.46, p. 81, Publication:01:04, Chalmers University of Technology, Sweden.
15. De Lorenzis, L. and Tepfers, R. (2003). A Comparative Study of Models on Confinement of Concrete Cylinders with Fiber-reinforced Polymer Composites, *ASCE J. Compos. Constr.*, **7**(3): 219–237.
16. Teng, J. G., Chen, J. F., Smith, S. T. and Lam, L. (2002). *FRP Strengthened RC Structures*, p. 245, John Wiley and Sons Ltd., Chichester, UK.
17. NF EN ISO 527-1 (1993). *Determination of Tensile Properties of Plastics Materials Part 1: General Principles*, p. 9, ISO International Standards.
18. NF EN ISO 527-2 (1993). *Determination of Tensile Properties of Plastics Materials Part 2: Test Conditions for Moulding and Extrusion Plastics,* p. 5, ISO International Standards.
19. NF EN ISO 527-5 (1997). *Determination of Tensile Properties of Plastics Materials Part 5: Test Conditions for Unidirectional Fibre-reinforced Plastic Composites,* p. 9, ISO International Standards.
20. Shahawy, M., Mirmiran, A. and Beitelman, T. (2000). Tests and Modeling of Carbon-wrapped Concrete Columns, *Composites Part B*, **31**(6): 471–480.
21. Richart, F. E., Brandtzaeg, A. and Brown, R. L. (1929). *The Failure of Plain and Spirally Reinforced Concrete in Compression,* Bulletin No.190, Engineering Experiment Station, University of Illinois, Urbana, USA.
22. Samaan, M., Mirmiran, A. and Shahawy, M. (1998). Model of Confined Concrete by Fiber Composites, *ASCE J. Struct. Eng.*, **124**(9): 1025–1031.
23. Saafi, M., Toutanji, H. A. and Li, Z. (1999). Behavior of Concrete Columns Confined with Fiber Reinforced Polymer Tubes, *ACI Mater. J.*, **96**(4): 500–509.
24. Spoelstra, M. R. and Monti, G. (1999). FRP-confined Concrete Model, *ASCE J. Compos. Constr.*, **3**(3): 143–150.
25. Matthys, S., Toutanji, H., Audenaert, K. and Taerwe, L. (2005). Axial Load Behavior of Large-scale Columns Confined with Fiber-reinforced Polymer Composites, *ACI Struct. J.*, **102**(2): 258–267.
26. Xiao, Y. and Wu, H. (2003). Compressive Behavior of Concrete Confined by Various Types of FRP Composite Jackets, *J. Reinf. Plast. Compos.*, **22**(13): 1187–1201.
27. Karbhari, V. M. and Gao, Y. (1997). Composite Jacketed Concrete under Uniaxial Compression – Verification of Simple Design Equations, *ASCE J. Mater. Civil Eng.*, **9**(4): 185–193.
28. Toutanji, H. (1999). Stress-Strain Characteristics of Concrete Columns Externally Confined with Advanced Fiber Composite Sheets, *ACI Mater. J.*, **96**(3): 397–404.
29. Jiang, T. and Teng, J. G. (2007). Analysis-oriented Stress-Strain Models for FRP-Confined Concrete, *Eng. Struct.*, **29**: 2968–2986.
30. Miyauchi, K., Inoue, S., Kuroda, T. and Kobayashi, A. (1999). Strengthening Effects of Concrete Columns with Carbon Fiber Sheet, *Trans. Jpn. Concr. Inst.*, **21**: 143–150.
31. Lam, L. and Teng, J. G. (2002). Strength Models for Fiber-reinforced Plastic Confined Concrete, *ASCE J. Struct. Eng.*, **128**(5): 612–623.
32. Lam, L. and Teng, J. G. (2003). Design-oriented Stress-Strain Model for FRP Confined Concrete, *Constr. Build. Mater.*, **17**: 471–489.
33. Wu, G., Lu, Z. T. and Wu, Z. S. (2006). Strength and Ductility of Concrete Cylinders Confined with FRP Composites, *Constr. Build. Mater.*, **20**: 134–148.
34. Ilki, A. (2006). FRP Strengthening of RC Columns (Shear, Confinement and Lap Splices), In: *Retrofitting of Concrete Structures by Externally Bonded FRPs*, Fib with Emphasis on Seismic Applications, Bulletin 35, pp. 123–142, Lausanne, Swiss.
35. Teng, J. G., Huang, Y. L., Lam, L. and Ye, L. P. (2007). Theoretical Model for Fiber Reinforced Polymer-confined Concrete, *ASCE J. Compos. Constr.*, **11**(2): 201–210.
36. Berthet, J. F., Ferrier, E. and Hamelin, P. (2006). Compressive Behavior of Concrete Externally Confined by Composite Jackets. Part B: Modeling, *Constr. Build. Mater.*, **20**: 338–347.
37. Theriault, M. and Neale, K. W. (2000). Design Equations for Axially-loaded Reinforced Concrete Columns Strengthened with FRP Wraps, *Can. J. Civil Eng.*, **27**(5): 1011–1020.
38. Yang, X., Nanni, A. and Chen, G. (2001). Effect of Corner Radius on the Performance of Externally Bonded Reinforcement, In: *Proceedings of the Fifth International Symposium on Fiber Reinforced Polymer for Reinforced Concrete Structures (FRPRCS-5)*, Cambridge, London, pp. 197–204.

39. Shehata, I. A. E. M., Carneiro, L. A. V. and Shehata, L. C. D. (2002). Strength of Short Concrete Columns Confined with CFRP Sheets, *RILEM Mater. Struct*., **35**: 50–58.
40. Vintzileou, E. and Panagiotidou, E. (2008). An Empirical Model for Predicting the Mechanical Properties of FRP Confined Concrete, *Constr. Build. Mater*., **22**: 841–854.
41. Fardis, M. N. and Khalili, H. H. (1982). FRP-encased Concrete as a Structural Material, *Mag. Concr. Res*., **34**(121): 191–202.
42. Rousakis, T. C. and Karabinis, A. I. (2008). Substandard Reinforced Concrete Members Subjected to Compression: FRP Confining Effects, *RILEM Mater. Struct*., **41**(9): 1595–1611.
43. Siddhawartha, M., Hoskin, A. and Fam, A. (2005). Influence of Concrete Strength on Confinement Effectiveness of Fiber-reinforced Polymer Circular Jackets, *ACI Struct. J*., **102**(3): 383–392.
44. Becque, J., Patnaik, A. and Rizkalla, S. H. (2003). Analytical Models for Concrete Confined with FRP Tubes, *ASCE J. Compos. Const*., **7**(1): 31–38.
45. Karabinis, A. I. and Rousakis, T. C. (2001). A Model for the Mechanical Behavior of the FRP Confined Columns, In: *Proceedings of the International Conference on FRP Composites in Civil Engineering*, Hong Kong, China, pp. 317–326.
46. Malvar, L. J., Morrill, K. B. and Crawford, J. E. (2004). Numerical Modeling of Concrete Confined by Fiber-reinforced Composites, *ASCE J. Compos. Constr*., **8**(4): 315–322.
47. Moran, D. A. and Pantelides, C. P. (2002). Variable Strain Ductility Ratio for Fiber Reinforced Polymer-confined Concrete, *ASCE J. Compos. Constr*., **6**(4): 224–232.
48. Lam, L., Teng, J. G., Cheung, C. H. and Xiao, Y. (2006). FRP-confined Concrete under Axial Cyclic Compression, *Cem. Concr. Compos*., **28**: 949–958.
49. Ilki, A., Kumbasar, N. and Koc, V. (2003). Low and Medium Strength Concrete Members Confined by Fiber Reinforced Polymer Jackets, *ARI: Bull. Istanbul Tech. Univ*., **53**(1): 118–123.